Can Polymer Solar Cells Open the Path to Sustainable and Efficient Photovoltaic Windows Fabrication?

著者（英）	Varun Vohra
journal or publication title	The Chemical Record
volume	19
number	7
page range	1166-1178
year	2019-07
URL	http://id.nii.ac.jp/1438/00008888/

doi: 10.1002/tcr.201800072

Can polymer solar cells open the path to sustainable and efficient photovoltaic windows fabrication?

Varun Vohra*[a]

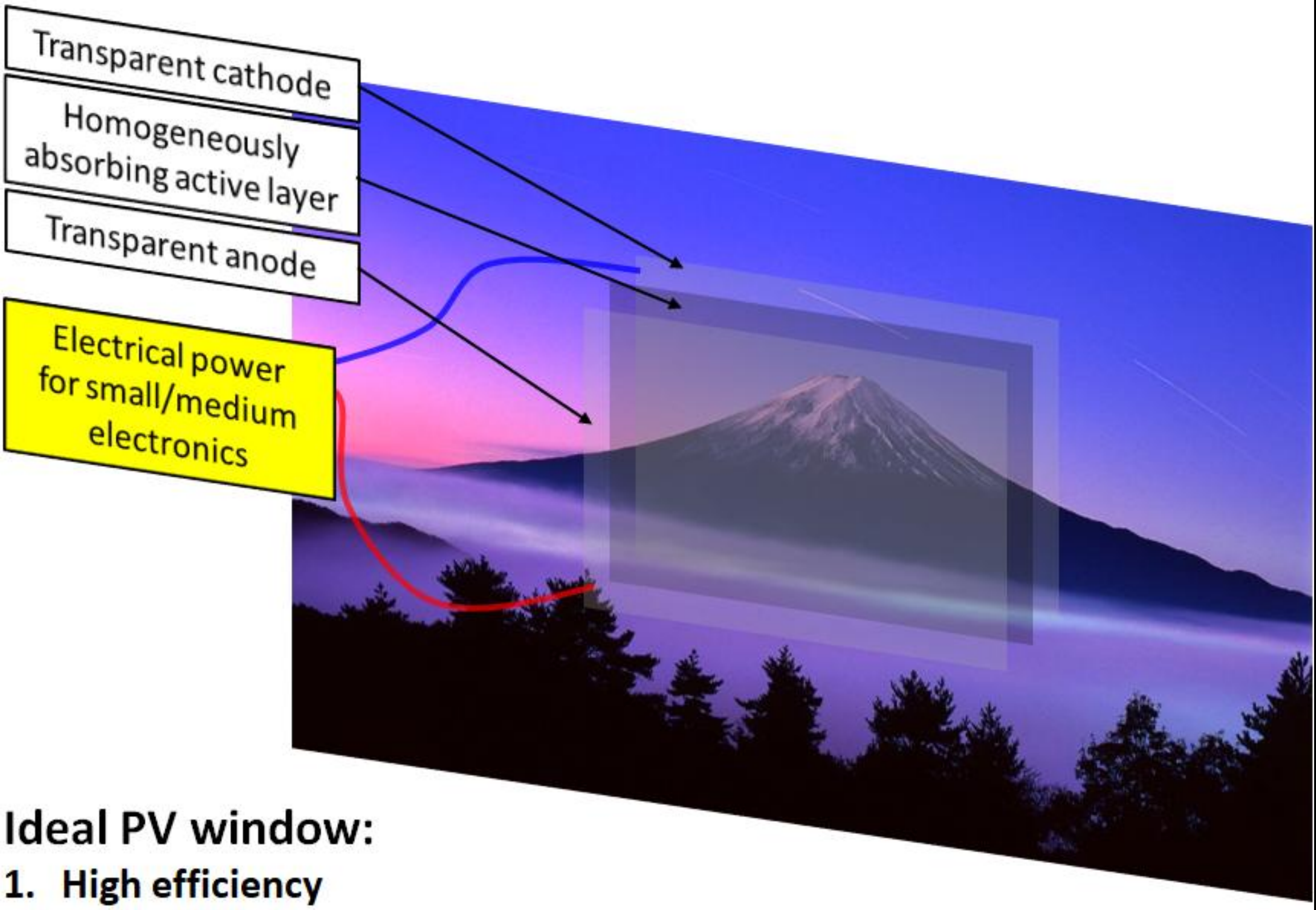

Ideal PV window:

1. **High efficiency**
2. **High color rendering index**
3. **High average visible transparency**
4. **Low-cost, eco-friendly and sustainable devices**

Abstract: Sunlight is among the most abundant energy sources available on our planet. Finding adequate solutions to properly and efficiently harvest it is of major importance to potentially solve the global energy crisis. Polymer solar cells have been introduced in the late 20th century as low-cost and easily processed alternative to the state-of-the-art silicon photovoltaics. Their power conversion efficiencies, which were initially rather low, are constantly improving and now reach values close to 15%. As their optical properties can be easily tuned, designing active layer which absorb homogeneously throughout the visible spectrum is relatively simple. These peculiar characteristics enable the possibility to fabricate visibly transparent solar cells with high color rendering indices which can be employed as photovoltaic windows. After reviewing some of the most successful examples of polymer solar cell-based transparent photovoltaic window fabrication, I will discuss the possibility to produce these devices in a sustainable and/or eco-friendly manner while maintaining their performances.

Varun Vohra received his PhD from the University of Milano-Bicocca (Italy) in 2009 for his study on organic semiconductor optoelectronics funded through a Marie Curie Fellowship. Between 2010 and 2014, he conducted research on polymer solar cells at the Japan Advanced Institute of Science and Technology, his host institution for the two JSPS Fellowships he secured in 2011 and 2012. Since 2014, he is Assistant Professor of Engineering Science at the University of Electro-communication where he leads a research group focusing on next-generation polymer technologies (polymer solar cells, polymer light-emitting devices and bio-inspired photonics). His contributions to the polymer photovoltaics field include pioneering works on devices with power conversion efficiencies over 10% and innovative green processes for efficient active layer fabrication.

1. Introduction

According to the International Energy Outlook published by the U.S. Energy Information Administration in September 2017,[1] the global energy consumption is predicted to increase by 28% before 2040. The use of renewable energy is foreseen to play an essential role to cope with this large demand in the near future. Consequently, finding innovative solutions to efficiently harvest the most abundant of these renewable energies, namely, solar energy, is an urgent matter. For the past couple of decades, a major effort is being made to replace the state-of-the-art silicon photovoltaic technologies with thin film solar cells to introduce innovative concepts such as transparent photovoltaic windows (PWs).[2] Although perovskite solar cells have a great potential for high efficiency semi-transparent PWs fabrication, polymer solar cells (PSCs) display the most promising capacity for high transmittance coupled with low-cost and sustainable (energy investment over return) device production. The device architecture of PSCs is fairly simple and composed of an active layer containing electron donor and electron acceptor materials sandwiched between two electrodes.[3] Indium tin oxide (ITO) is commonly employed as a transparent bottom electrode while the top electrodes are generally fabricated by thermal evaporation of metals. However, some researchers argue that ITO is becoming scarcer in the Earth's crust and consequently alternative transparent conductive electrodes (TCEs) have been receiving a growing interest over the past few years as some can potentially be deposited using low-cost and sustainable processes.[4-7] As these TCEs have been carefully reviewed recently, I will only mention them when they are applied to the fabrication of the PSCs mentioned in this review. In fact, the electrodes are not the only part of the PSCs that should remain visibly transparent. To produce PSCs with high transmittance and color rendering indices (CRIs), a particular attention should be given to the active layer. The strategies to ensure that efficient PSCs can be produced while maintaining high CRIs and average visible transparencies (AVTs) will be presented in the following section of this Personal Account.

Unlike other emerging photovoltaic technologies and their relatively continuous performance growth, PSCs demonstrate a step-like increase in performances closely linked to major breakthroughs in chemistry such as the introduction of thiophene-based polymers,[8] donor-acceptor p-type polymers[9] or non-fullerene acceptors.[10,11] After showing how the tunable optoelectronic properties of organic semiconductors can be efficiently employed to develop new strategies for PW production with high CRIs, I will present several studies in which PSCs with relatively high CRIs or AVTs were successfully fabricated. In Section 3, I will discuss the sustainability and eco-friendliness of the PSC active layer fabrication processes. In fact, the method commonly employed for active layer production, namely, spin-coating from chlorinated solutions, considerably reduces the sustainability of these photovoltaic devices. Sustainable fabrication of efficient PWs is of critical importance to ensure that PSC-based technologies continue to develop in the future and consequently, I will discuss recently introduced strategies to reduce or eliminate the use of chlorinated solvents during active layer deposition.

2. Active materials for visibly transparent PSC fabrication

To fabricate transparent or semi-transparent devices with high CRIs, two main strategies can be employed based on the sunlight irradiance spectrum reaching the surface of the Earth (AM1.5g, Figure 1(a)). The first one consists in using active materials that do not absorb in the visible but only absorb light in

---

[a] Dr. V. Vohra
Department of Engineering Science
University of Electro-communications
1-5-1 Chofugaoka, Chofu City, Tokyo, 182-8585 Japan
E-mail: varun.vohra@uec.ac.jp

the ultraviolet (UV) and/or the infra-red (IR) regions. The second approach uses a combination of active materials that, when blended together, homogeneously absorbs throughout the visible. Despite the fact that this will result in a reduction in AVT, the observed colors through the PSC should remain unchanged (high CRIs). Facile tuning of the organic semiconductor optoelectronic properties through simple chemistry thus becomes a major advantage to explore these strategies and select the one(s) more adapted for high performance PSC-based PW fabrication (Figure 1(b)).

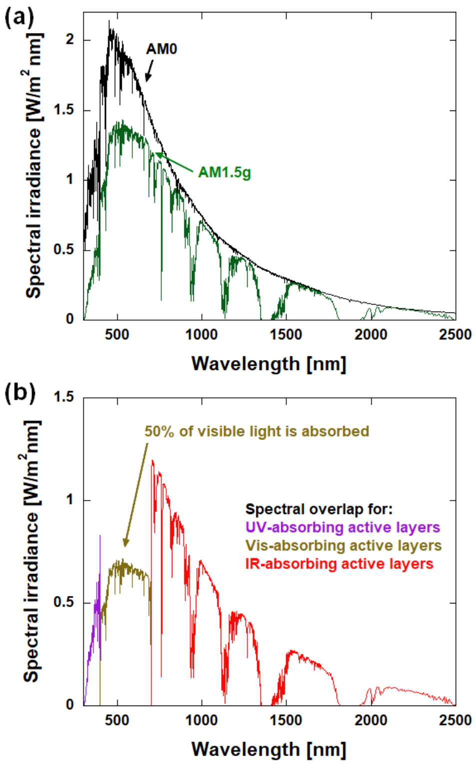

Figure 1. (a) Solar spectra measured for Air Mass Zero (AM0) and at the surface of the Earth (AM1.5g); (b) Available solar irradiance for UV-absorbing, Vis-absorbing (AVT~50%) and IR-absorbing active layers.

2.1. Why are IR absorbing PSCs more promising than UV absorbing ones?

HOMO and LUMO levels of polymer semiconductors are highly affected by the chemical structure of the monomer and the number of repeating units which define the electron delocalization (conjugation length) in the molecule.[12,13] For example, thiophene monomers have a large bandgap over 4 eV but increasing the molecule length to 6 repeating units or to thiopene-based polymers results in decreased bandgap values of 2.2 and 2 eV, respectively. Similar bandgap reductions with increasing chain length are seen in all conjugated polymers where conjugation occurs along the backbone. Consequently, UV-absorbing wide bandgap organic semiconductors are usually small molecules or polymers in which the conjugation is confined within a single monomer. Among the widely employed polymer semiconductors, poly(9-vinylcarbazole) (PVK) is one of the few materials in which conjugation is confined within its pending groups and not in the polymer backbone. The large optical bandgap of PVK (~3.6 eV) makes it ideal for UV-absorbing (sub-400 nm) PSCs. Nonetheless, despite its low lying HOMO which can yield large open-circuit voltages (Voc), very few attempts have been made to fabricate PVK-based PSCs.[14] Both organic and hybrid PVK-based solar cells produce very low short-circuit densities (Jsc) which is due to the small amount of light available for harvesting in the sub-400 nm region of the solar spectrum (AM1.5g).[14,15] In addition, PSC architectures are usually based on ITO-covered glass coated with zinc oxide (ZnO) or poly(3,4-ethylenedioxythiophene) polystyrene sulfonate (PEDOT:PSS) and all these materials absorb below 400 nm. UV-only absorbing active layers are consequently not generally used in PSCs. Note that the most commonly employed electron acceptor ([6,6]-Phenyl-C$_{61}$-butyric acid methyl ester, PC$_{61}$BM) absorbs principally in the UV which suggests that the low performances obtained with PVK may also be related to its low hole mobility.

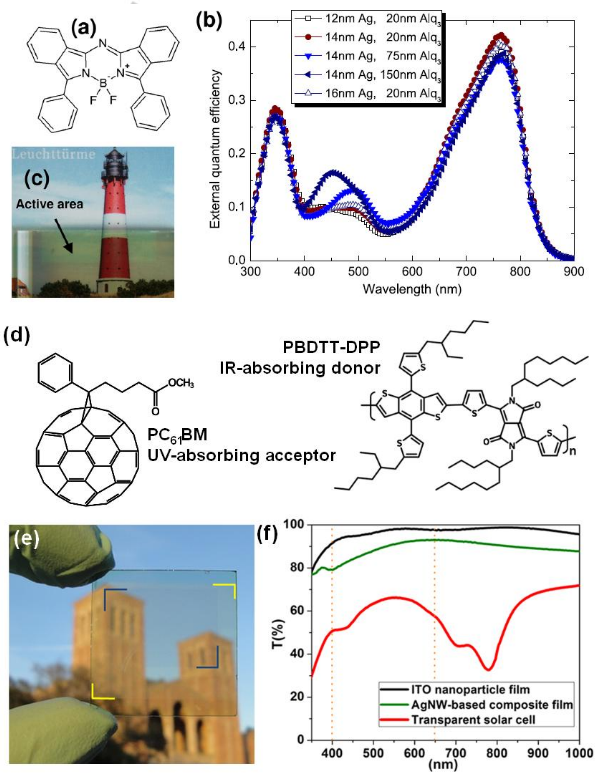

Figure 2. (a) Molecular structure of benzannulated difluoro-bora-bis-(1-phenyl-indoyl)-azamethine and (b) the EQE and (c) photograph of transparent PSCs employing it as active material. Adapted with permission from [16], Copyright 2011, American Institute of Physics. (d) Active molecules employed in PC$_{61}$BM:PBDTT-DPP PSCs; (e) photographs and (f) transmittance spectra of the devices. Adapted with permission from [17], Copyright 2012, American Chemical Society.

IR-absorbing active layers do not suffer from parasitic absorbance (glass, ITO, ZnO, PEDOT:PSS) and their spectral overlap with AM1.5g is extremely large (Figure 1(b)) which suggests that they could produce efficient transparent PWs. In fact, using a small molecule IR absorber (Figure 2(a)) combined with C_{60} fullerene acceptors, Meiss *et al*. fabricated quasi-transparent evaporated solar cells with Jsc up to 5 mA/cm^2.[16] Their spectral contributions to the Jsc (external quantum efficiency, EQE, in Figure 2(b)) clearly demonstrate that for the optimized electron transporting layer and electrode thicknesses, current is generated principally from sub-400 nm and over 600 nm light. As part of the visible light (400 ~ 700 nm) is absorbed, a small color variation can be observed in Figure 2(c) between the area in the photograph with and without device. Similar results were obtained by Chen *et al.* with a polymer absorbing in the IR region (PBDTT-DPP, chemical structure in Figure 2(d)) combined with $PC_{61}BM$, which absorbs in the UV.[17] The photograph taken through the transparent PSC (Figure 2(e)) suggests that they yield high CRIs. Additionally, high AVTs over 50% (Figure 2(f)) could be produced when employing PBDTT-DPP:$PC_{61}BM$ active layers combined with ITO and silver nanowire-based TCEs.

Molecules with Narrow bandgaps below 1.5 eV absorbing in the IR/NIR are produced by extending conjugation in the molecular structure designs.[18-20] The concept of alternating electron donating-electron accepting (ED-EA) units is now widely employed to tune the HOMO-LUMO bandgap and optoelectronic properties of conjugated molecules and can serve the purpose of producing low bandgap active materials.[21-24] The building blocks for these copolymers are generally 5 or 6 member aromatic rings which can include heteroatoms. Benzenes, thiophenes, carbazoles or thiadiazoles are among the most commonly employed building blocks which are linked through C-C bonds or fused in the final molecular structure. Despite the fact that this strategy remarkably decreases the HOMO-LUMO bandgap, as both ED and EA contribute to the absorption properties of the copolymers, producing copolymers absorbing solely in the IR region is quite challenging.[22-25] Li *et al*. selected two IR absorbing materials, PTB7-Th as electron donor and BT-CIC as electron acceptor (chemical structures in Figure 3(a)), to fabricate transparent devices.[26] They were able to produce PSCs with a high PCE of 11.2% (Figure 3(b)) with 100 nm-thick Ag anodes and devices with a CRI of 91 with 10 nm-thick transparent Ag electrodes (Figure 3(c), 3(d) and 3(e)). Figures 3(b) and 3(c) show that the sub-700 nm absorption has a non-negligible contribution to the device performances which strongly affects the transmission of red colors (above 600 nm). This visible absorption from the active layer considerably reduces the AVT of the devices and the non-uniform transmittance through the PSC yields relatively low CRIs (Figure 3(e)). Nonetheless, these promising results with Jsc over 15 mA/cm^2 for devices with 10 nm-thick Ag anodes confirm that harvesting sunlight in the IR region is a more efficient strategy than UV-absorbing active layers for PSCs. With future developments in chemistry, we can expect to see the rise of molecules that will only absorb in the IR region to produce PWs with high transmittance and high CRIs. However, considering the large library of available polymer donors and fullerene or non-fullerene acceptors absorbing in the visible, finding the right combination of donor and acceptor materials to homogeneously absorb throughout the visible seems to be the adequate approach.

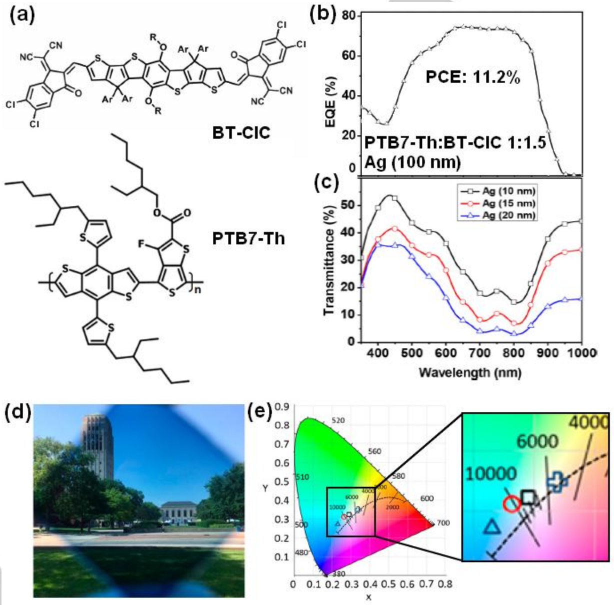

Figure 3. (a) Molecular structures of active molecules employed in PTB7-Th:BT-CIC PSCs, (b) the EQE and (c) transmittance of the devices as well as (d) a photograph and (e) the CIE coordinates of the semi-transparent PSCs. Adapted with permission from [26], Copyright 2017, American Chemical Society.

2.2. A compromise between high performances and high AVT in uniformly absorbing PSCs

P3HT:$PC_{61}BM$ active layers, which were once the reference active materials for PSCs have now become obsolete.[8] Their performances are largely overcome by ED-EA copolymers combined with fullerenes absorbing in the visible ([6,6]-Phenyl-C_{71}-butyric acid methyl ester, $PC_{71}BM$) or non-fullerene acceptors such as ITIC (Figure 4(a)).[27-31] In fact, the P3HT:$PC_{61}BM$ pair was far from being ideal for the fabrication of PWs with high CRIs (Figure 4(b)). On the other hand, ITIC has an absorption spectrum that is complementary to that of P3HT and P3HT:ITIC active layers absorb light relatively homogeneously from 400 to 700 nm (Figure 4(c)).[30] Unfortunately, the PCE of P3HT:ITIC PSCs active layers is relatively low (~2.25%). When ITIC is associated with low bandgap copolymers such as PBDB-T (Figure 4(a)), PCEs over 10% are produced but relatively low CRIs are to be expected.[31] In fact, several studies have demonstrated that semi-transparent PSCs with PCEs and AVTs over 7% and 25%, respectively, can be produced employing non-fullerene acceptors.[19,32-34] However, these high performance semi-transparent PSCs exhibit a colored glass aspect confirming that they are not the ideal candidates for high CRIs PWs. Low bandgap polymers such as PBDB-T combined with $PC_{71}BM$ display a higher potential when it comes to producing uniformly absorbing devices provided that the adequate donor:acceptor ratio is found (Figure 4(d)).

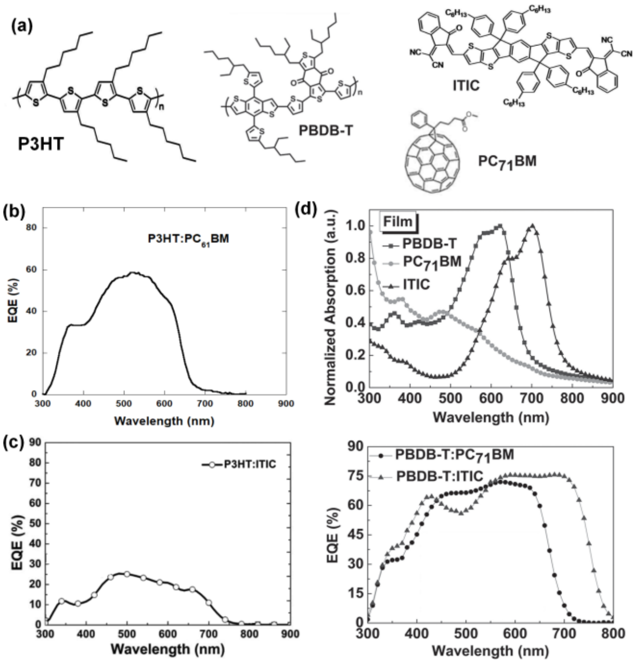

Figure 4. (a) Molecular structures of P3HT, PBDB-T, ITIC and $PC_{71}BM$. EQEs of (b) P3HT:$PC_{61}BM$ and (c) P3HT:ITIC PSCs. Adapted with permission from [30], Copyright 2018, Wiley-VCH. (d) Absorption spectra of PBDB-T, $PC_{71}BM$ and ITIC as well as EQE of PBDB-T:$PC_{71}BM$ and PBDB-T:ITIC PSCs. Adapted with permission from [31], Copyright 2016, Wiley-VCH.

Although the PTB7-Th:$PC_{71}BM$ devices prepared by Wong *et al*. yielded relatively low CRIs of 87.1 (Figure 5(a)),[35] Shen *et al*. recently managed to considerably increase that value (Figure 5(b)).[36] The authors employ photonic crystals acting as Bragg reflectors to balance the transmitted colors and increase the CRI of their reference device (CRI = 91) up to 95 while maintaining an AVT of 20%. However, starting with active layers that homogeneously absorb throughout the visible will remove the necessity for additional photonic crystal-like structures engineering. This was successfully achieved using thin films based on PTB7 and $PC_{71}BM$ as they exhibit perfectly complimentary absorptions in the visible (Figure 6(a)).[37,38]

When a 1:1.5 donor:acceptor ratio is employed, relatively flat absorption profiles are generated from PTB7:$PC_{71}BM$ from 400 to 700 nm. The inverted architecture PSCs fabricated by Liu *et al*. using graphene anodes exhibit an AVT of approximately 40% (Figures 6(b)) and high CRIs (Figure 6(c)).

Wong *et al*. studied various combinations of conjugated polymer donor:$PC_{71}BM$ and obtained the highest CRI (95.4) with PBDTTT-CT as the electron donor (Figure 7(a)).[35] However, to obtain efficient devices with PCEs of 5.2%, they employed relatively thick silver electrodes (20 nm) resulting in a low AVT of 14%. Using the same donor:acceptor pair and 18 nm-thick Ag electrodes, Chen *et al*. fabricated PSCs with a PCE, CRI and AVT of 6.22%, 97.3 and 21.3%, respectively.[39] In fact, they confirmed that a balance between electrode conductivity (thicker Ag) and optical transparency (thin Ag) has to be found to produce devices with high AVT and CRI while retaining high performances (Figure 7(b)). The 18 nm-thick Ag electrode devices have a PCE only 18% lower than the reference devices fabricated with 60 nm-thick anodes which produce a PCE of 7.56%.

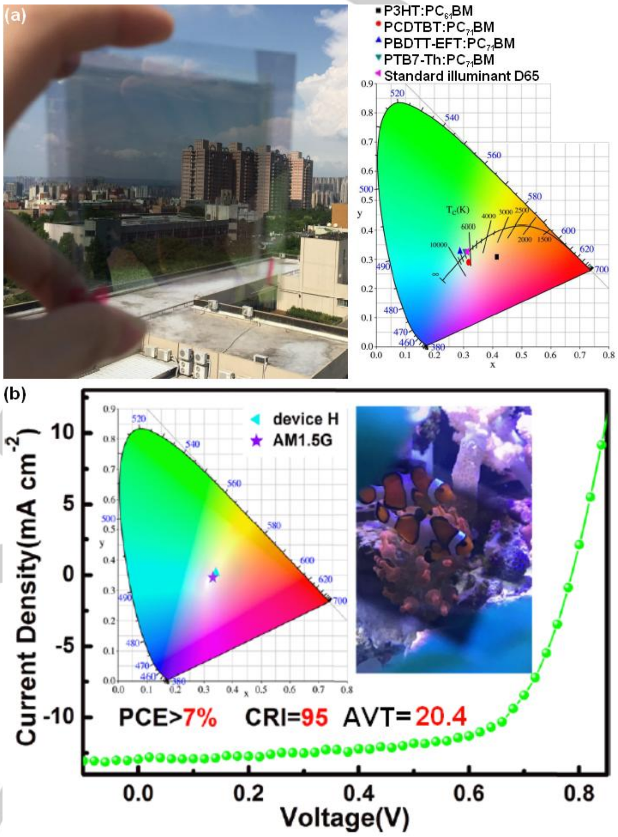

Figure 5. (a) Photograph and CIE coordinates of PTB7-Th:$PC_{71}BM$ PSCs. Adapted with permission from [35], Copyright 2017, Elsevier B.V. (b) CIE coordinates, photograph and J-V curves of PTB7-Th:$PC_{71}BM$ PSCs employing photonic crystals as Bragg reflectors. Adapted with permission from [36], Copyright 2018, American Chemical Society.

Using ternary blend active layers or tandem structures are efficient methods to increase to fabricate high performance PSCs.[40,41] These strategies also enable the possibility to further adjust the optical properties of the devices which should enable producing devices with high PCEs and CRIs employing non-fullerene acceptors. Including photonic crystals within the device architecture for light manipulation can enhance the PSC performances but generally leads to a reduction in transmitted light.[36,42,43] Furthermore, to ensure that PSC-based PWs are one day commercialized, other aspects have to be taken into account such as the production cost and the sustainability of the fabrication process.[44] In Section 3, I will review some techniques for eco-friendly and sustainable active layer fabrication.

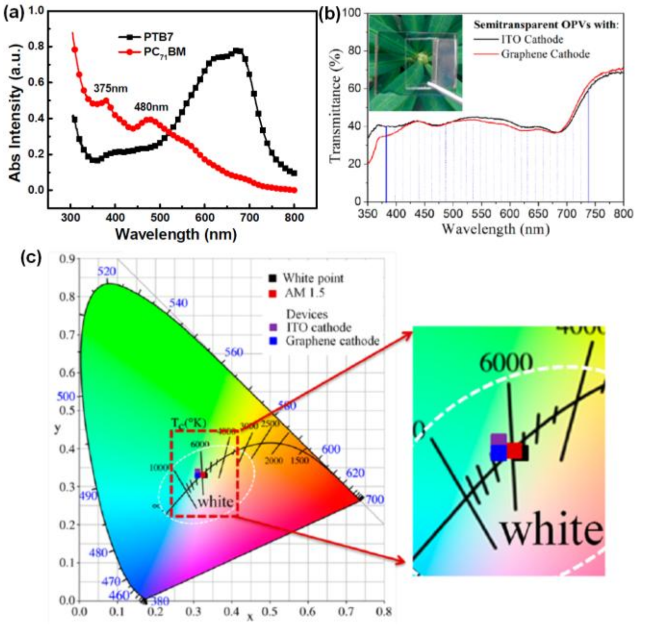

Figure 6. (a) Absorption spectra of PTB7 and $PC_{71}BM$ films. Adapted with permission from [38], Copyright 2015, Royal Society of Chemistry; (b) transmittance and (c) CIE coordinates of the PTB7:$PC_{71}BM$ PSCs. The inset of Figure 6(b) corresponds to a photograph of the PSC. Adapted with permission from [37], Copyright 2015, American Chemical Society.

3. Eco-friendly and sustainable active layer fabrication processes

Most high performance active layers are produced using chlorinated aromatic solvents which are harmful to the environment and the human health. To deal with this issue, several "green" solvents and additives have been proposed such as toluene, *o*-xylene (*o*-XY), 1,2,4-trimethylbenzene (TMB), mesitylene (MS), 1-methylnaphthalene (MN), 1,2-dimethylnaphthalene (1,2-DMN), acetophone (AP), N-methyl-pyrrolidone (NMP) or carbon disulphide (CS_2) to replace the chlorobenzene (CB) and 1,2-dichlorobenzene (DCB).[45] Tables 1 and 2 summarize the hazard data collected using the safety data sheets for each solvent from Sigma-Aldrich.

Looking at the potential hazards to human health and/or the environment, there does not seem to be a substantial difference among these solvents. MN, 1,2-DMN and AP are relatively uncommon solvents and the hazard statements list for these solvents might not be complete (as mentioned on their safety sheets). Although the hazard statements suggest otherwise, many authors have categorized CB as hazardous while toluene is listed among the green solvents. Both toluene and *o*-XY, the most commonly employed solvents for "green" fabrication of PSCs are categorized extremely harmful if swallowed or when they enter airways. Most solvents listed as green might be slightly better than DCB but this is also arguable and would benefit from further experimentation on MN, 1,2-DMN and AP.

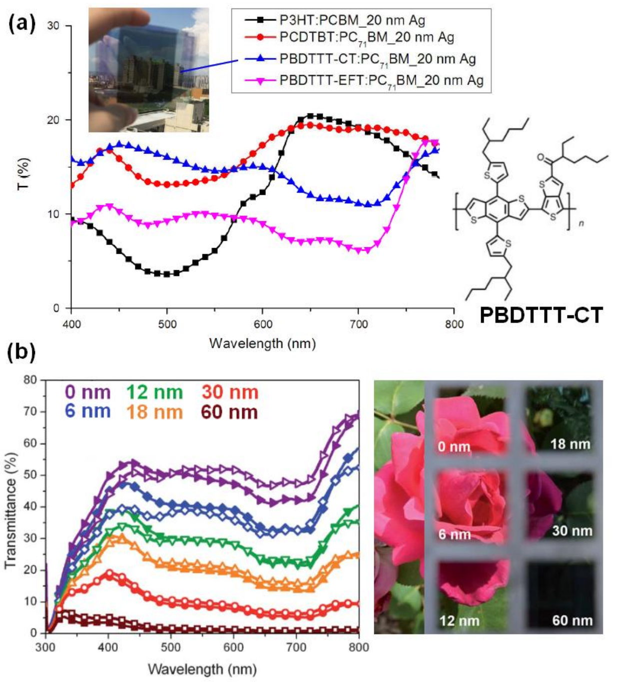

Figure 7. (a) Various active layers studied in reference [35] together with the molecular structure of PBDTTT-CT and the photograph of a PBDTTT-CT:$PC_{71}BM$ PSC (inset). Adapted with permission from [35], Copyright 2017, Elsevier B.V. (b) Transmittance of PBDTTT-CT:$PC_{71}BM$ PSCs fabricated with various Ag electrode thicknesses ranging from 0 to 60 nm and their corresponding photographs. Adapted with permission from [39], Copyright 2012, Royal Society of Chemistry.

Table 1. Description of the hazard statements listed in **Table 2**.

Hazard Statement	Risk
H225, H226, H227	Flammable/combustible liquid/vapour
H302	Harmful if swallowed
H304	May be fatal if swallowed or enters airways
312	Harmful in contact with skin
H315, H317	Causes skin irritation/allergic reaction
H318	Damages the eye
H319	Causes eye irritation
H332	Harmful if inhaled
H335	May cause respiratory irritation
H336	May cause drowsiness or dizziness
H360, H361	Damage fertility/unborn child
H372	Toxic to organs
H401,H410, H411, H412, H441	Toxic to aquatic life

Table 2. List of hazard statements for “hazardous” and “green” solvents employed for PSC active layer fabrication.

Solvent	Hazard statements (category[a], target if any)
“hazardous”	
CB	H226(3), H315(4), H332(2), H441(2)
DCB	H227(4), H302(4), H315(2), H317(1), H319(2A), H332(4), H335(3), H410(1)
“green”	
toluene	H225(2), H304(1), H315(2), H336(3, central nervous system), H361(2), H373(2), H401(2)
o-XY	H226(3), H304(1), H312(4), H315(2), H319(2A), H332(4), H335(3, respiratory system), H412(3)
TMB	H226(3), H304(4), H315(2), H319(2A), H332(3, respiratory tract), H335(1), H411(2)
MS	H226(3), H304(1), H315(2), H319(2A), H335(3, respiratory system), H401(2), H411(2)
MN	H302(4), H411(2)*
1,2-DMN	Data unavailable (toxic to aquatic life)*
AP	H227(4), H302(4), H318(1)*
NMP	H227(4), H315(2), H319(2A), H335(3, respiratory system) H360(1B)
CS_2	H225(2), H315(2), H319(2A), H332(4), H361(2), H372(1, respiratory system), H401(2)

[a] hazard intensity from various categories: 1>2>3>4; A>B

* incomplete set of data

Consequently, rather than employing arguably greener solvents for active layer fabrication, using water or ethanol (EtOH) would represent real eco-friendly solutions to active layer deposition. Alternatively, considerably reducing the amount of solvent used for the deposition process and/or enable the possibility to recycle it would make active layer fabrication much more eco-friendly and sustainable.

3.1. Can efficient PSCs be produced using active layers deposited from water?

Semiconducting polymers are essentially apolar and unsoluble. To solubilize their backbones in organic solvents such as CB or DCB, they are functionalized with alkyl, alkyl halide, ether or ester groups or can be fluorinated. Since the pioneering study by Zhao *et al.* in 2009, a large number of water or EtOH-soluble conjugated polymers have been synthesized and applied in PSCs as cathode buffer layers.[46-48] Synthesis of water or EtOH-soluble conjugated polymers was achieved by functionalizing their side chains with amino, phosphate, carboxyl or sulfonyl groups which provides them with amphiphilic properties. Despite the fact that these polymers become fairly soluble in water, they have only been applied as active layer material in a single publication.[49] Lanzi *et al*. synthesized two P3HT derivatives which contain a sodium sulfonate group (PT6S) and a trimethylammonium bromide group (PT6N), respectively (Figure 8(a)). Their reference P3HT:$PC_{61}BM$ PSCs yield a PCE of 3.6% while the PT6S and PT6N-based ones exhibit lower values of 1.59% and 2.93%, respectively. The authors suggest that $PC_{61}BM$ is readily soluble in water. However, it is likely that the water-soluble polymers act as surfactants to generate micellar aggregates composed of both donor (outer shell in contact with water) and acceptor molecules (inside the micelle). Nguyen *et al*. produced active layers using EtOH-soluble polymer and C_{60} derivatives that yield PCEs up to 0.75% and exhibit a highly crystalline yet well-mixed active layer morphology.[50] Employing polymers such as PT6S and PT6N associated with water-soluble fullerenes such as the PEGylated C60 might be an efficient method to produce water-soluble active layers for eco-friendly PSC fabrication (PEG-C60, Figure 8(a)).[51]

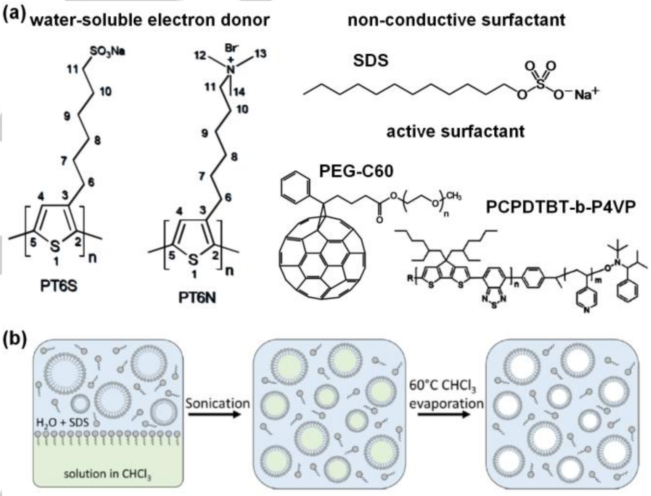

Figure 8. (a) Chemical structures of water-soluble electron donors, non-conductive and electrically active surfactants for eco-friendly PSC fabrication. Adapted with permission from [49], Copyright 2017, Elsevier B.V. (b) Schematic representation of the miniemulsion process. Adapted with permission from [55], Copyright 2017, American Chemical Society.

In fact, PEG-C60 has been employed to generate donor-acceptor blend nanoparticles (NPs) formed in water through the miniemulsion process which exhibit enhanced charge separation properties.[51] Landfester *et al*. were actually the first to introduce the miniemulsion process based on non-conducting surfactants, sodium dodecyl sulfate (SDS, Figure 8(a)), for the formation of conjugated polymer-based water-dispersed NPs (Figure 8(b)).[52] Although most attempts to fabricate PSCs using water-processed NPs (WPNPs) lead to low PCEs (<1%),[53,54] a few successful examples of efficient devices can also be found in literature.[55-60] To achieve high performances, the electrically insulating SDS is removed prior to active layer deposition and the NP dispersion is concentrated to ensure that closely packed NP films are formed. D’Olieslaeger *et al*. annealed the WPNP films at 180°C for 20 min to form continuous active layers that produce PCEs of 3.8%, a value much lower than the PSCs produced using chlorinated solvents (PCE~6.1%). To avoid high temperature annealing, Bag *et al*. deposited a thin layer of $PC_{61}BM$ from dichloromethane on top of the NP layer.[56] Annealing at high temperatures considerably reduces the sustainability of the process while on the other hand, deposition of $PC_{61}BM$ from dichloromethane slightly decreases its eco-friendliness.

To avoid the SDS removal step, we developed electrically active copolymers composed of a conjugated rod (PCPDTBT) covalently bond to a water-soluble flexible coil (P4VP) (Figure 8(a)).[61] Vinylpyridine provides the block copolymer with amphiphilic properties and should mix well with fullerene derivatives.[62.63] We produced active layers from spin-coated PCPDTBT-b-P4VP:$PC_{61}BM$ WPNPs annealed at temperatures lower than 100°C yielding a PCE of 0.52%, which is much lower than PCPDTBT:$PC_{61}BM$ device performances found in literature (PCE ~ 3%).[64,65] Spin-coating an additional drop of $PC_{61}BM$ dichloromethane solution on the NP active layer improved the PCE to 2.53%. This value is only 15% lower than conventional devices but only 1/5th of chlorinated solvent employed.

The reprecipitation technique is a surfactant-less alternative to miniemulsion proposed by Gärtner *et al*. which uses EtOH or methanol (MetOH) as the non-solvent.[66] A P3HT:ICBA solution from chloroform is slowly injected into MetOH to form the NP suspension after evaporation of chloroform. Schwarz *et al*. and Gärtner *et al*. both argued that better mixing of P3HT and $PC_{61}BM$ or ICBA can be achieved in NPs prepared using reprecipitation compared to miniemulsion.[67,68] The as cast P3HT:ICBA NP PSCs have low PCEs of 0.1% which can be gradually increased to 1.2%, 3.0%, 3.7% and 3.9% by applying thermal annealing at 100°C, 150°C, 180°C and 200°C, respectively. The high temperatures employed to produce efficient devices considerably decrease the device sustainability and MetOH is still strongly hazardous to human health. However, Gärtner *et al*. also produced devices with PCEs up to 3.5% using EtOH which is much less hazardous to human health. Multilayer P3HT:ICBA active layers produced through sequential deposition of NP from EtOH further improves the PCE to 4.2% using a lower annealing temperature of 150°C.[69] Using water as non-solvent for reprecipitation produced low PCEs below 0.2% after annealing at 160°C suggesting that EtOH might be a much better option when it comes to the fabrication of efficient PSCs from eco-friendly nanoparticle dispersions.[70]

Although the above mentioned methods considerably reduce the amount of hazardous solvent employed, the necessary time to fabricate the devices is largely increased. Furthermore, most of these eco-friendly solvent formulations are still deposited using spin-coating which generates a large amount of active materials waste and increases the production cost. It is therefore important to assess which deposition process should be employed to replace spin-coating when it comes to low-cost, sustainable and eco-friendly device fabrication.

3.2. Selecting the adequate low-cost and sustainable active layer deposition method

Several roll-to-roll compatible deposition processes such as blade-coating, slot-die coating, screen printing and inkjet printing have been developed over the past decade to replace spin-coating and reduce the amount of wasted material during PSC active layer deposition.[71] Despite the fact that slot-die coating and blade-coating have similar film formation kinetics, PSCs fabricated by blade-coating generally exhibit higher performances as compared to slot-die coated ones.[35,72-75] Recently, unconventional techniques such as electrospray deposition and push-coating have demonstrated their potential for high performance device fabrication.[76-82] Here, I will compare the methods that yield relatively high PCEs, namely, spin-coating, blade-coating, electrospray deposition and push-coating, in terms of cost reduction, environment-friendliness and sustainability (Figure 9).

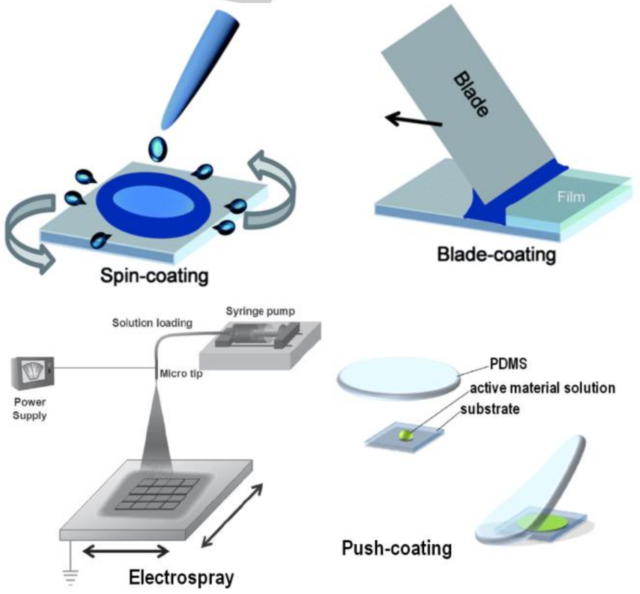

Figure 9. Schematic representations of the processes compared in this paper, namely, spin-coating, blade-coating, electrospray deposition and push-coating. Adapted with permissions from [72], [76] and [79]. Copyrights 2016, Royal Society of Chemistry; 2010, Wiley-VCH; 2017, American Chemical Society.

As electrospray and push-coating are relatively unexplored processes, to ensure that the various deposition techniques mentioned above can be quantitatively compared, I will focus on results obtained with P3HT:$PC_{61}BM$ active layers. However, as these alternative low-cost deposition techniques are gradually becoming more popular, we should expect similar comparative studies applied to higher efficiency active layers in the future.

Wong *et al*. compared P3HT:$PC_{61}BM$ active layers deposited by spin-coating and blade coating in regular device architectures which produced PCEs of 3.9 and 3.5%, respectively.[35] In addition to being much more suitable for large area uniform thin film deposition, blade-coating exhibits the potential for reduction in volume of solution employed during the process. Spin-coating is typically performed using 100 μl of 40 mg/ml CB solution while for blade-coating only 50 μl are used. Blade-coating consequently halves the amount of active materials and hazardous solvent used for the active layer deposition and is thus slightly more eco-friendly and lower-cost compared to spin-coating. The coating speed (200 mm/s) that the authors employed generates uniform films through fast drying when active layers are deposited on substrates at a temperature of 80°C. Unlike spin-coating, no further annealing step at 140°C for 20 min is necessary to obtain PCEs of 3.5%. Consequently, the much lower thermal input necessary (80°C 1s as compared to 140°C 20 min) also makes blade-coating more sustainable than spin-coating from an energy input point-of-view. A closer look at the photovoltaic parameters of spin-coating and blade-coating suggest that a higher crystallinity and larger phase separation is obtained for annealed spin-coated films confirming that blade-coating remains a relatively fast drying process when operated under the above mentioned conditions.

Electrospray is a process that was first introduced for nuclear research in 1957 and is currently considered as a low-cost continuous deposition process for organic electronics.[83] In 2010, Kim *et al*. first applied electrospray to P3HT:PC$_{61}$BM PSC active layers to produce devices with PCEs up to 3.25% after solvent vapor soaking with CB and thermal annealing at 160°C for 15 min.[76] Despite the highly inhomogeneous topology of the electrosprayed active layers, the resulting PSCs exhibited a PCE only slightly lower than those of spin-coated ones (3.62%). Unfortunately, the amount of solution used for deposition is not described in that study but the authors argue that 16 substrates (of unknown dimensions) can be deposited contemporarily. Electrospraying is generally performed with low concentration P3HT:PC$_{61}$BM solutions (0.5~2.2 mg/ml).[76-78] These are much lower than the concentrations employed for spin-coating (16~40 mg/ml) which may induce the reader into believing that this deposition method considerably reduces the amount of active material. According to Shah *et al*., the amount of 0.5 mg/ml solution necessary to deposit a 110 nm-thick active layer is 2 ml (20 and 40 times larger volumes than spin-coating and blade-coating, respectively).[78] The total active material amount thus becomes 1 mg which corresponds to roughly 1/4th of that employed for spin-coating. Electrospraying consequently has the potential to reduce the cost for active layer fabrication by a factor of 4 but the hazardous solvent amount is 20 times larger than for spin-coating which considerably reduces the eco-friendliness and sustainability of the process. Takahira *et al*. demonstrated that electrosprayed PSCs can be fabricated using non-halogenated solvents such as *o*-XY, which brings us back to the discussion on eco-friendliness of "green" solvents. We should also keep in mind that, unlike the mini-emulsion process presented in the previous section, spin-coating, blade-coating or electrospray do not enable the possibility to collect and recycle the hazardous solvent used during thin film production. This is also true for other deposition methods like slot-die coating, screen printing and inkjet printing. Combining mini-emulsions with one of the above mentioned coating processes (e.g., electrospray) could provide the adequate method to contemporarily reduce the production cost and increase the eco-friendliness and sustainability of the device fabrication.

On the other hand, push-coating is a relatively new coating process that allows for eco-friendly and low-cost fabrication of organic electronic devices.[79-82] Push-coated films are produced by depositing a very small amount of solution on a substrate (less than 5 μl for covered areas of 5 cm^2) on which a polydimethylsiloxane (PDMS)-based elastomer is placed. The solution spreads through capillary forces over the desired area and a thin wet film is formed. The solvent then diffuses inside the elastomer to form homogeneous thin films whose thickness can be controlled by the solution concentration. It was first introduced by Ikawa *et al*. for the fabrication of large scale P3HT-based thin film transistors.[81] Kobayashi *et al.* then successfully fabricated push-coated PSCs with much lower PCE values as compared to spin-coated ones.[82] This first study on push-coated PSCs used extremely thin PDMS films which likely induced the formation of non-uniform active layers due to PDMS buckling upon exposure to chlorinated solvent. In fact, even when additional weight was placed on top of the PDMS film to ensure that flat PTB7:PC$_{71}$BM active layers are produced, the PCE of these push-coated PSCs only reached values of 2.65%. We demonstrated that efficient PSCs and OLEDs as well as nanopixel OLEDs can be fabricated by push-coating when thick PDMS layers are employed.[79,80] In fact, Ikawa *et al.* had already suggested that the important parameter to control push-coating are the elastomer film's solvent retention properties.[81] The mm-thick PDMS layers we produced for push-coating have good mechanical stability even when exposed to large amounts of chlorinated solvents which facilitates their handling and removes the necessity for additional weight. Furthermore, as the hazardous solvents are temporarily trapped inside the thick PDMS, their recovery and recycling can be achieved relatively easily. In addition to large reduction in employed amounts of solvent and active material during push-coating (Table 3), P3HT:PC$_{61}$BM active layers push-coated at 50°C for 5 min produce similar PCEs compared to spin-coated PSCs annealed at 140°C for 10 min. We recently fabricated push-coated with higher performing active materials that display PCEs up to 5.3% (results not published) which also confirm that push-coating is a versatile process with a great potential for low-cost roll-to-roll fabrication of high efficiency PSCs in a sustainable and eco-friendly manner. However, push-coating does have its limits. It can only be employed with solvents that diffuse inside PDMS which excludes water and other eco-friendly solvents such as EtOH. Consequently, unlike blade-coating or electrospray, there is no possibility to combine push-coating with the miniemulsion or reprecipitation processes or to use push-coating for water/alcohol charge selection layer deposition (e.g., PEDOT:PSS, PFN). Given the extremely small amount of hazardous solvent employed during push-coating and the fact that it can be easily recycled, not being able to combine it with eco-friendly formulations is not a major issue. However, to produce all-push-coated regular devices, we will have to either find new materials acting as hole transporting layers which are soluble in solvents that diffuse into PDMS or fabricate devices without PEDOT:PSS. We demonstrated that PEDOT:PSS-less

(ITO-only) push-coated PSCs yield PCEs of 3.1% (93% of the PCE obtained with PEDOT:PSS layers) which could be an interesting research direction to pursue in the future as removing the acidic PEDOT:PSS layer would also highly enhance the long-term device stability.

Table 3 summarizes the data collected on the three deposition processes discussed here. Compared to traditional spin-coating, blade-coating reduces the amount of hazardous solvents and active material by half. It is roll-to-roll compatible which makes it more adequate than spin-coating for large-scale device production. Electrospray further reduces the amount of employed material to 1/4th and simultaneous deposition of multiple devices seems to be possible. However, the amount of used hazardous solvent and the necessary high annealing temperatures considerably decrease the eco-friendliness and sustainability of electrosprayed PSCs. Push-coating pushes the boundaries of cost reduction to a maximum as the amount of material for active layer fabrication is approximately 30 and 15 times lower than blade-coating and electrospray, respectively. Similarly, push-coating employs an extremely small amount of hazardous solvents and active layers can be produced at lower temperatures than the two other techniques. The solvent can be easily collected and recycled making the push-coating process almost completely sustainable while maintaining high device performances.

Table 3. Summary of cost reduction, eco-friendliness and sustainability aspects of alternative deposition processes for PSC fabrication together with their relative PCE compared to spin-coated reference devices.

Process	Blade-coating	Electro-spray	Push-coating
Active material (mg)	2	1	0.06
Hazardous solvent (μl)	50	2000	3
Process temperature (°C)	80	160	50
Solvent recycling ability	No	No	Yes
relative PCE (%)[a]	90	90	101

[a] relative to spin-coated devices from the same study

4. Conclusions

In summary, in this Personal Account, we discussed the various possibilities in terms of material design and process to fabricate efficient and visibly transparent PSCs through low-cost, eco-friendly and sustainable process. A large number of active molecules (donor and acceptors) have recently been introduced to improve the performances of PSCs. To produce devices with high CRIs, the first method is to employ active materials that absorb only in the UV or IR regions. Despite the fact that this approach can theoretically yield high AVTs and CRIs, they have not been extensively studied. This is because on one hand, the UV contribution from the solar spectrum reaching Earth is relatively small, while on the other hand it is difficult to synthesize IR absorbing materials that do not also absorb in the visible. Using materials that complimentary and uniformly absorb throughout the visible increased the PCEs and CRIs of transparent PSCs but the AVTs of these devices were much lower than those produced using the first strategy. Furthermore, simultaneously obtaining high CRIs and PCEs can be challenging as the adequate donor:acceptor ratio for high efficiency does not always correspond to that necessary to produce uniform absorption throughout the visible. Nonetheless, devices with PCEs over 5% and CRIs over 95% could be produced using relatively thin Ag layers as electrode. In fact, a compromise has to be found between device performances and the amount of light transmitted.

To produce the transparent PSCs in a low-cost, eco-friendly and sustainable manner, the commonly employed method (spin-coating from halogenated solvents) should be replaced with “greener” processes. Although toluene and *o*-XY have been proposed as alternative “green” solvents for efficient PSC fabrication, their safety data sheets suggest that they are as hazardous as CB when it comes to human health and aquatic environment. WPNP or EtOH-dispersed NP active layers are a more sustainable and green fabrication approach and I hope that we will soon find the solutions to obtain the adequate morphologies to enhance their photovoltaic performances while avoiding the use of high temperature annealing. As an alternative strategy, developing new roll-to-roll-compatible deposition processes which considerably reduce the amount of solvent and active materials could also highly increase the sustainability and eco-friendliness of PSCs while simultaneously reducing their fabrication cost. Among the various processes discussed here, push-coating has the most promising potential as it considerably reduces the amounts of active material and hazardous solvent to a strict minimum. The solvent trapped within PDMS can easily be recovered and recycled. The low temperature required for efficient PSC fabrication also contributed to increasing the sustainability of push-coated PSCs. Works on eco-friendly processes applied to transparent PWs fabrication are still rather limited but as the PSC field further develops, I hope to see a growing number of devices with high PCEs, AVTs and CRIs produced by sustainable processes.

Acknowledgements

The experimental studies presented in this Personal Account (WPNPs and push-coating) were supported by the Japan Society for the Promotion of Science through the Grant-in-aid for Young Scientists (B) program (Grant No. 17K14549) and the JGC-S (Nikki-Saneyoshi) Scholarship Foundation.

Keywords: Polymer Solar Cells • Conjugated Polymers • Renewable Energy • Fullerenes • Donor-acceptor system

References

[1] International Energy Agency. *World Energy Outlook.* OECD Publishing, Paris, **2017**.

[2] J. Sun, J.J. Jasieniak, J. Phys. D **2017**, *50*, 093001.

[3] P.R. Berger, M. Kim, *J. Renew. Sustain. Energy* **2018**, *10*, 013508.

[4] Y. W. Li, G. Y. Xu, C. H. Cui, Y. F. Li, *Adv. Energy Mater.* **2018**, *8*, 1701791.

[5] D. S. Hecht, L. Hu, G. Irvin, *Adv. Mater.* **2011**, *23*, 1482-1513.

[6] S. Lu, Y. Sun, K. Ren, K. Liu, Z. Wang, S. Qu, *Polymers* **2018**, *10*, 5.

[7] M. Luo, Y. Liu, W. Huang, W. Qiao, Y. Zhou, Y. Ye, L.-S. Chen, *Micromachines* **2017**, *8*, 12.

[8] M. T. Dang, L. Hirsch, G. Wantz, *Adv. Mater.* **2011**, *23*, 3597-3602.

[9] Y. Gao, M. Liu, Y. Zhang, Z. Liu, Y. Yang, L. Zhao, *Polymers* **2017**, *9*, 39.

[10] W. Chen, Q. Zhang, *J. Mater. Chem. C* **2017**, *5*, 1275-1302.

[11] C. Yan, S. Barlow, Z. Wang, H. Yan, A.K.-Y. Jen, S.R. Marder, X. Zhan, *Nat. Rev. Mater.* **2018**, *3*, 18003.

[12] U. Salzner, J.B. Lagowski, P.G. Pickup, R.A. Poirier, *Synth. Met.* **1998**, *96*, 177-189.

[13] J. Gierschner, J. Cornil, H.-J. Egelhaaf. *Adv. Mater.* **2007**, *19*, 173-191.

[14] L. Chen, L. Yang, M. Shi, H. Chen, *Sol. Energy Mater. Sol. Cells* **2010**, *94*, 2244-2250.

[15] A. Benchaabane, Z.B. Hamed, A. Telfah, M.A. Sanhoury, F. Kouki, K. Zellama, H. Bouchriha, *Mat. Sci. Semicon. Proc.* **2017**, *64*, 115-123.

[16] J. Meiss, F. Holzmueller, R. Gresser, K. Leo, M. Riede, Appl. Phys. Lett. **2011**, *99*, 193307.

[17] C.-C. Chen, L. Dou, R. Zhu, C.-H. Chung, T.-B. Song, Y.B. Zheng, S. Hawks, G. Li, P.S. Weiss, Y. Yang. *ACS Nano* **2012**, *6*, 7185-7190.

[18] X. Li, H. Huang, H. Bin, Z. Peng, C. Zhu, L. Xue, Z.-G. Zhang, Z. Zhang, H. Ade, Y. Li, *Chem. Mater.* **2017**, *29*, 10130-10138.

[19] H. Huang, X. Li, L. Zhong, B. Qiu, Y. Yang, Z.-G. Zhang, Z. Zhang, Y. Li, *J. Mater. Chem. A* **2018**, *6*, 4670-4677.

[20] X. Li, T. Yan, H. Bin, G. Han, L. Xue, F. Liu, Y. Yi, Z.-G. Zhang, T.P. Russell, Y. Li, *J. Mater. Chem. A* **2017**, *5*, 22588-22597.

[21] T. Xu, L. Yu, *Mater. Today* **2014**, *17*, 11-15.

[22] Y. Cao, J.-H. Dou, N.-J. Zhao, S. Zhang, Y.-Q. Zheng, J.-P. Zhang, J.-Y. Wang, J. Pei, Y. Wang. *Chemistry of Materials* **2017**, *29*, 718-725.

[23] K. Brymora, L. Ducasse, A. Delaure, L. Hirsch, T. Jarrosson, C. Niebel, F. Serein-Spirau, R. Peresutti, O. Dautel, F. Castet, *Dyes Pigm.* **2018**, *149*, 882-892.

[24] K. Kawabata, M. Saito, I. Osaka, K. Takimiya, *J. Am. Chem. Soc.* **2016**, *138*, 7725-7732.

[25] Y. Lin, J. Wang, Z. Zhang, H. Bai, Y. Li, D. Zhu, X. Zhan, *Adv. Mater.* **2015**, *27*, 1170-1174.

[26] Y. Li, J.-D. Lin, X. Che, Y. Qu, F. Liu, L.-S. Liao, S.R. Forrest, *J. Am. Chem. Soc.* **2017**, *139*, 17114-17119.

[27] V. Vohra, K. Kawashima, T. Kakara, T. Koganezawa, I. Osaka, K. Takimiya, H. Murata. *Nat. Photonics* **2015**, *9*, 403-408.

[28] J. Hou, O. Inganäs, R.H. Friend, F. Gao, *Nat. Mater.* **2018**, *17*, 119-128.

[29] S. Q. Zhang, Y. P. Qin, J. Zhu, J. H. Hou, *Adv. Mater.* **2018**, 30, 1800868.

[30] Y. Qin, M.A. Uddin, Y. Chen, B. Jang, K. Zhao, Z. Zheng, R. Yu, T.J. Shin, H.Y. Woo, J. Hou, *Adv. Mater.* **2016**, *28*, 9416-9422.

[31] W. Zhao, D. Qian, S. Zhang, S. Li, O. Inganäs, F. Gao, J. Hou, *Adv. Mater.* **2016**, *28*, 4734-4739.

[32] M.B. Upama, M. Wright, N.K. Elumalai, M.A. Mahmud, D. Wang, C. Xu, A. Uddin, *ACS Photonics* **2017**, *4*, 2327-2334.

[33] H. Yang, Y. Wu, Y. Zou, Y. Dong, Y. Yuan, C. Cui, Y. Li, *J. Mater. Chem. A* **2018**, *6*, 14700-14708.

[34] S. Dai, X. Zhan, *Adv. Energy Mater.* **2018**, *8*, 1800002.

[35] Y.Q. Wong, H.-F. Meng, H.Y. Wong, C.S. Tan, C.-Y. Wu, P.-T. Tsai, C.-Y. Chang, S.-F. Horng, H.-W. Zan, *Org. Electron.* **2017**, *43*, 196-206.

[36] P. Shen, G. Wang, B. Kang, W. Guo, L. Shen, *ACS Appl. Mater. Interfaces* **2018**, *10*, 6513-6520.

[37] Z. Liu, P. You, S. Liu, F. Yan, *ACS Nano* **2015**, *9*, 12026-12034.

[38] D. Huang, Y. Li, Z. Xu, S. Zhao, L. Zhao, J. Zhao, *Phys. Chem. Chem. Phys.* **2015**,*17*, 8053-8060.

[39] K.-S. Chen, J.-F. Salinas, H.-L. Yip, L. Huo, J. Hou, A.K.-Y. Jen, *Energy Environ. Sci.* **2012**, *5*, 9551-9557.

[40] W. Huang, P. Cheng, Y. Yang, G. Li, Y. Yang, *Adv. Mater.* **2018**, *30*, 1705706.

[41] C.-Y. Chang, L. Zuo, H.-L. Yip, Y. Li, C.-Z. Li, C.-S. Hsu, Y.-J. Cheng, H. Chen, A.K.-Y. Jen, *Adv. Funct. Mater.* **2013**, *23*, 5084-5090.

[42] Y. Chen, M. Elshobaki, Z. Ye, J.-M. Park, M.A. Noack, K.-M. Ho, S. Chaudhary. *Phys. Chem. Chem. Phys.* **2013**,*15*, 4297-4302.

[43] L. Zhou, Q.-D. Ou, J.-D. Chen, S. Shen, J.-X. Tang, Y.-Q. Li, S.-T. Lee, *Sci. Rep.* **2014**, *4*, 4040.

[44] C. J. Brabec, *Sol. Energy Mater. Sol. Cells* **2004**, *83*, 273-292.

[45] S. Zhang, L. Ye, H. Zhang, J. Hou, *Mater. Today* **2016**, *19*, 533-543.

[46] Y. Zhao, Z. Xie, C. Qin, Y. Qu, Y. Geng, L. Wang, *Sol. Energy Mater. Sol. Cells* **2009**, *93*, 604-608.

[47] W. Lee, J.H. Seo, H.Y. Woo, *Polymer* **2013**, *54*, 5104-5121.

[48] C. Duan, K. Zhang, C. Zhong, F. Huang, Y. Cao, *Chem. Soc. Rev.*, **2013**, *42*, 9071-9104.

[49] M. Lanzi, E. Salatelli, L. Giorgini, A. Mucci, F. Pierini, F.P. Di-Nicola, *Eur. Polym. J.* **2017**, *97*, 378-388.

[50] T.L. Nguyen, C. Lee, H. Kim, Y. Kim, W. Lee, J.H. Oh, B.J. Kim, H.Y. Woo, *Macromolecules* **2017**, *50*, 4415-4424

[51] Y. J. Kim, B. Lee, *ChemSusChem* **2018**, *11*, 1628.

[52] K. Landfester, R. Montenegro, U. Scherf, R. Güntner, U. Asawapirom, S. Patil, D. Neher, T. Kietzke, *Adv. Mater.* **2002**, *14*, 651-655.

[53] T.R. Andersen, T.T. Larsen-Olsen, B. Andreasen, A.P.L. Böttiger, J.E. Carlé, M. Helgesen, E. Bundgaard, K. Norrman, J.W. Andreasen, M. Jørgensen, F.C. Krebs, *ACS Nano* **2011**, *5*, 4188-4196.

[54] T. Kietzke, D. Neher, K. Landfester, R. Montenegro, R. Güntner, U. Scherf, *Nat. Mater.* **2003**, *2*, 408-412.

[55] F.J.M. Colberts, M.M. Wienk, R.A. Janssen, *ACS Appl. Mater. Interfaces* **2017**, *9*, 13380-13389.

[56] M. Bag, T.S. Gehan, L.A. Renna, D.D. Algaier, P.M. Lahti, D. Venkataraman, *RSC Adv.* **2014**, *4*, 45325-45331.

[57] C. Xie, A. Classen, A. Späth, X. Tang, J. Min, M. Meyer, C. Zhang, N. Li, A. Osvet, R.H. Fink, C.J. Brabec, *Adv. Energy Mater.* **2018**, *8*, 1702857.

[58] L. D'Olieslaeger, M. Pfannmöller, E. Fron, I. Cardinaletti, M. Van Der Auweraer, G. Van Tendeloo, S. Bals, W. Maes, D. Vanderzande, J. Manca, A. Ethirajan, *Sol. Energy Mater. Sol. Cells* **2017**, *159*, 179-188.

[59] L. D'Olieslaeger, G. Pirotte, I. Cardinaletti, J. D'Haen, J. Manca, D. Vanderzande, W. Maes, A. Ethirajan, *Org. Electron.* **2017**, *42*, 42-46.

[60] L. Parrenin, G. Laurans, E. Pavlopoulou, G. Fleury, G. Pecastaings, C. Brochon, L. Vignau, G. Hadziioannou, E. Cloutet, *Langmuir* **2017**, *33*, 1507-1515.

[61] S. Zappia, G. Scavia, A. M. Ferretti, U. Giovanella, V. Vohra, S. Destri, *Adv. Sustainable Syst.* **2018**, *2*, 1700155.

[62] V. Gernigon, P. Lévêque, F. Richard, N. Leclerc, C. Brochon, C.H. Braun, S. Ludwigs, D.V. Anokhin, D.A. Ivanov, G. Hadziioannou, T. Heiser, *Macromolecules* **2013**, *46*, 8824-8831.

[63] H.J. Kim, J.-H. Kim, J.-H. Ryu, Y. Kim, H. Kang, W.B. Lee, T.-S. Kim, B.J. Kim, *ACS Nano* **2014**, *8*, 10461-10470.

[64] D. Muhlbacher, M. C. Scharber, M. Morana, Z. Zhu, D. Waller, R. Gaudiana, R. C. J. Brabec, *Adv. Mater.* **2006**, *18*, 2884-2889.

[65] M. Morana, M. Wegscheider, A. Bonanni, N. Kopidakis, S. Shaheen, M. Scharber, Z. Zhu, D. Waller, R. Gaudiana, C.J. Brabec, *Adv. Funct. Mater.* **2008**, *18*, 1757-1766.

[66] S. Gärtner, M. Christmann, S. Sankaran, H. Röhm, E. Prinz, F. Penth, A. Pütz, A.E. Türeli, B. Penth, B. Baumstümmler, A. Colsmann, *Adv. Mater.* **2014**, *26*, 6653-6657.

[67] K.N. Schwarz, S.B. Farley, T.A. Smith, K.P. Ghiggino, *Nanoscale* **2015**,*7* ,19899-19904.

[68] S. Gärtner, A.J. Clulow, I.A. Howard, E. P. Gilbert, P.L. Burn, I.R. Gentle, A. Colsmann, *ACS Appl. Mater. Interfaces* **2017**, *9*, 42986-42995.

[69] S. Gärtner, S. Reich, M. Bruns, J. Czolk, A. Colsmann, *Nanoscale* **2016**, *8*, 6721-6727.

[70] G. Prunet, L. Parrenin, E. Pavlopoulou, G. Pecastaings, C. Brochon, G. Hadziioannou, E. Cloutet, *Macromol. Rapid Commun.* **2018**, *39*, 1700504.

[71] R. Søndergaard, M. Hösel, D. Angmo, T.T. Larsen-Olsen, F. C. Krebs, *Mater. Today* **2012**, *15*, 36-49.

[72] K. Zhao, H. Hu, E. Spada, L.K. Jagadamma, B. Yan, M. Abdelsamie, Y. Yang, L. Yu, R. Munie, R. Li, G.O. Ngongang Ndjawa, A. Amassian, *J. Mater. Chem. A* **2016**, *4*, 16036-16046.

[73] Z. Peng, Y. Zhang, Y. Xia, K. Xiong, C. Cai, L. Xia, Z. Hu, K. Zhang, F. Huang, L. Hou, *J. Mater. Chem. A* **2015**, *3*, 20500-20507.

[74] J. Yang, Y. Lin, W. Zheng, A. Liu, W. Cai, X. Yu, F. Zhang, Q. Liang, H. Wu, D. Qin, L. Hou, *ACS Appl. Mater. Interfaces* **2018**, *10*, 22485-22494.

[75] H.W. Ro, J.M. Downing, S. Engmann, A.A. Herzing, D.M. DeLongchamp, L., J. Richter, S. Mukherjee, H. Ade, M. Abdelsamie, L.K. Jagadamma, A. Amassian, Y. Liu, H. Yan. *Energy Environ. Sci.* **2016**, *9*, 2835-2846.

[76] J. Kim, W. Chung, K. Kim, D.Y. Kim, K. Paeng, S.M. Jo, S. Jang, *Adv. Funct. Mater.* **2010**, *20*, 3538-3546.

[77] K. Takahira, A. Toda, K. Suzuki, T. Fukuda, *Phys. Status Solidi A* **2017**, *214*, 1600536.

[78] S.K. Shah, R. Gunnella, L. Hirsch, M. Abbas. *Thin Solid Films* **2017**, *640*, 104-108.

[79] V. Vohra, W. Mróz, S. Inaba, W. Porzio, U. Giovanella, F. Galeotti, *ACS Appl. Mater. Interfaces* **2017**, *9*, 25434-25444.

[80] V. Vohra, F. Galeotti, U. Giovanella, W. Mróz, M. Pasini, C. Botta, *ACS Appl. Mater. Interfaces* **2018**, *10*, 11794-11800.

[81] M. Ikawa, T. Yamada, H. Matsui, H. Minemawari, J. Tsutsumi, Y. Horii, M. Chikamatsu, R. Azumi, R. Kumai, T. Hasegawa, *Nat. Comm.* **2012**, *3*, 1176.

[82] S. Kobayashi, D. Kaneto, S. Fujii, H. Kataura, Y. Nishioka, *J. Chin. Adv. Mater. Soc.* **2015**, *3*, 1-8.

[83] D.J. Carswell, J. Milsted, *J. Nucl. Energy* **1957**, *4*, 51-54.

Entry for the Table of Contents

PERSONAL ACCOUNT

Polymer solar cells are low-cost and easily processed alternative to silicon photovoltaics. Their power conversion efficiencies are constantly improving and now reach values close to 15%. As their optical properties can be easily tuned, designing active layer which absorb homogeneously throughout the visible spectrum is relatively simple and enable the possibility to fabricate visibly transparent solar cells which can be employed as photovoltaic windows. Here, we will discuss whether efficient transparent polymer solar cells can be fabricated through sustainable and/or eco-friendly processes.

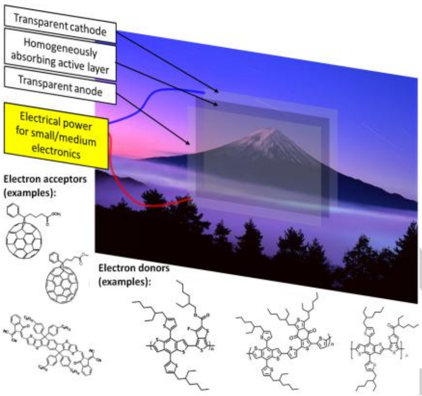

*Varun Vohra**

Page No. – Page No.

Can polymer solar cells open the path to sustainable and efficient photovoltaic windows fabrication?